A Paradigm Change: Efficient Transfection of Human Leukemia Cells by Stimuli-Responsive Multicompartment Micelles

Alexandra C. Rinkenauer,[†,‡] Anja Schallon,[†,‡] Ulrike Günther,[†,‡] Michael Wagner,[†,‡] Eva Betthausen,[§] Ulrich S. Schubert,[†,‡,*] and Felix H. Schacher[†,‡,*]

[†]Laboratory of Organic and Macromolecular Chemistry (IOMC), Friedrich Schiller University Jena, Humboldtstrasse 10, 07743, Jena, Germany, [‡]Jena Center for Soft Matter (JCSM), Friedrich Schiller University Jena, Philosophenweg 7, 07743 Jena, Germany, and [§]Macromolecular Chemistry II, Bayreuth Center for Colloids and Interfaces, University Bayreuth, 95440 Bayreuth, Germany

ABSTRACT The controlled nonviral delivery of genetic material using cationic polymers into cells has been of interest during the past three decades, yet the ideal delivery agent featuring utmost transfection efficiency and low cytotoxicity still has to be developed. Here, we demonstrate that multicompartment micelles from stimuli-responsive triblock terpolymers, polybutadiene-*block*-poly(methacrylic acid)-*block*-poly(2-(dimethylamino)ethyl methacrylate) (BMAAD), are promising candidates. The structures exhibit a patchy shell, consisting of amphiphilic (interpolyelectrolyte complexes, MAA and D) and cationic patches (excess D), generating a surface reminiscent to those of certain viruses and capable of undergoing pH-dependent changes in charge stoichiometry. After polyplex formation with plasmid DNA, superior transfection efficiencies can be reached for both adherent cells and human leukemia cells. Compared to the gold standard PEI, remarkable improvements and a number of advantages were identified for this system, including increased cellular uptake and an improved release of the genetic material, accompanied by fast and efficient endosomal escape. Furthermore, high sedimentation rates might be beneficial regarding *in vitro* applications.

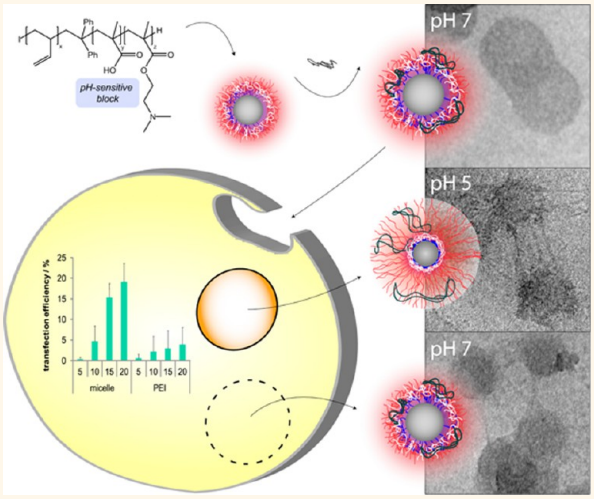

KEYWORDS: multicompartment micelles · interpolyelectrolyte complexes · nonviral gene transfection · polyplexes · human leukemia cells

The controlled delivery of genetic material into eukaryotic cells has been the focus of interdisciplinary scientific activities during the last three decades.[1,2] Within the field of nanomedicine, successful nonviral gene delivery holds great promise for the treatment of a wide variety of diseases, as a suitable transfection agent,[3] once identified, might be used in different approaches. Besides evolutionary qualified and very efficient viral transfection, nonviral delivery is of high interest, reflected in the large number of nonviral transfection agents being proposed. Thereby, among polymeric materials, poly(ethylene imine) (PEI) represents the "gold standard" for *in vitro* applications.[4]

The efficient protection of nucleic acids like plasmid DNA (pDNA) during delivery while maintaining utmost biocompatibility is one of the key requirements for such materials. In general, cationic polyelectrolytes are capable of forming polyplexes with negatively charged pDNA, the main driving forces being electrostatic interactions and a gain in entropy for the whole system.[5,6] Polyplexes with an excess of positive charges support both protection against degradation and uptake *via* the negatively charged cell membrane. Several studies show that the polymer architecture and the overall molar mass have a major influence on the transfection efficiency (TE).[7,8] Nevertheless, it is still

* Address correspondence to ulrich.schubert@uni-jena.de, felix.schacher@uni-jena.de.

Received for review April 25, 2013 and accepted October 22, 2013.

Published online October 22, 2013
10.1021/nn402072d

challenging to design systems comprising high TE and low cytotoxicity for gene delivery applications, as in the case of most cationic polymers, like PEI, high TEs are accompanied by increasing cytotoxicity. The use of poly(ethylene glycol) (PEG) as, *e.g.*, biocompatible shell is one straightforward approach to decrease the cytotoxicity but usually leads to lower TE.[9,10]

In addition, up to now most nonviral transfection agents fail in case of suspension cells, *e.g.*, Jurkat T cells, a model cell line for human leukemia cells. This has been attributed to the fact that 3D cultivation decreases the contact probability between cells and polyplexes in general, if compared to the mechanism proposed for the transfection of adherent cells.[11,12] Hence, designing polymers that are capable of efficient gene transfer into suspension cells would allow targeting immune cells for the therapy of immune defects (*e.g.*, HIV), for cancer (*e.g.*, leukemia), or to improve transient transfection in biotechnological approaches.[13] All these issues are further impeded by the fact that the underlying transfection mechanism for pDNA in contrast to siRNA (short interfering RNA) is far from being completely understood, rendering the design of efficient transfection agents for this purpose extraordinarily difficult.[14,15]

Here, we demonstrate for the first time the advantage of pH-responsive multicompartment micelles formed *via* self-assembly of a stimuli-responsive triblock terpolymer, polybutadiene-*block*-poly(methacrylic acid)-*block*-poly(2-(dimethylamino)ethyl methacrylate) (BMAAD, PB_{800}-*b*-$PMAA_{200}$-*b*-$PDMAEMA_{285}$; the subscripts denote the degrees of polymerization; the overall molar mass of BMAAD is 105 300 g/mol), as promising transfection agents for pDNA. Multicompartment structures represent a unique class of materials where either core, shell, or corona are further subdivided. Several strategies have been used to induce compartmentalization in block copolymer derived materials, including combinations of highly incompatible segments, kinetic control, or stepwise self-assembly by applying solvent mixtures.[16−18] Although multicompartment architectures have been in the focus for more than two decades, applications have been scarcely demonstrated. One very elegant example, however, was shown by Lodge and co-workers, where the segregated domains within micellar cores could be used to store two different hydrophobic guest molecules.[19] Regarding pH-responsive micellar carriers as gene delivery vehicles, pioneering work was performed by Kataoka and co-workers. For example, they used ABC triblock terpolymers with two cationic segments of different pK_a, facilitating the disruption of the endosome upon decrease of the pH[20] or, in another example, segments which underwent charge conversion during the uptake process.[21] Also, the use of pH-sensitive linkers between unlike segments of AB diblock copolymers has proven to be advantageous.[22]

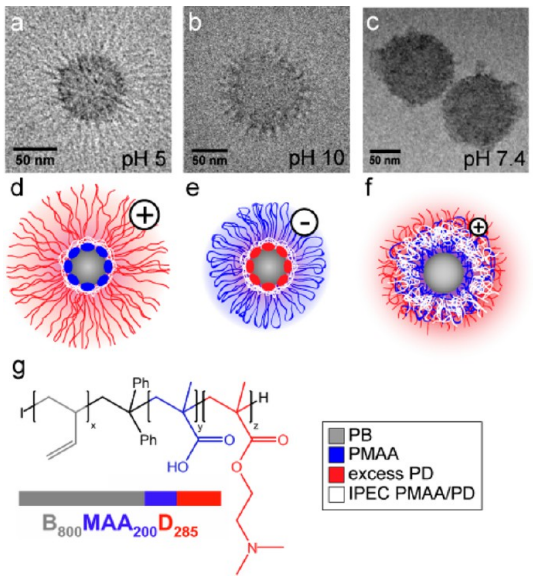

Figure 1. Cryo-TEM micrographs and schematic depictions of BMAAD micelles at pH 5 (a, d), pH 10 (b, e), and pH 7.4 (c, f). Structure and block lengths of the used BMAAD triblock terpolymer (g). Cryo-TEM images of pure BMAAD (a, b, c) and schematic illustrations thereof (d, e, f).

The aim of this work was to investigate how the rather heavy and voluminous BMAAD micelles can be used as efficient and pH-responsive nonviral gene transfection agents for adherent cells and human T-lymphocytes. We were interested whether the presence of different surface patches, also known from viral structures (*e.g.*, alpha viruses),[23−25] influences important process bottlenecks such as cytotoxicity or carrier/serum interaction. Further, insights into the underlying mechanism for pDNA transfection (which is far from being completely understood) by using a combination of different analytical techniques including asymmetric flow field-flow fractionation (AF4), cryogenic electron microscopy (cryo-TEM), analytical ultracentrifugation (AUC), and confocal laser scanning microscopy (CLSM) are presented.

RESULTS AND DISCUSSION

In our case, for BMAAD (PB_{800}-*b*-$PMAA_{200}$-*b*-$PDMAEMA_{285}$), the hydrophobic PB forms the micellar core, which, at low pH, is surrounded by a PMAA shell and a PDMAEMA corona (Figure 1). Such micelles are dynamic and show a strong pH-dependence concerning their shape, size, and surface charge.[26] At endosomal pH (∼ 5), PMAA is uncharged, and PDMAEMA forms a cationic corona (Figure 1a and d), whereas at pH 10, PDMAEMA is uncharged and partially collapsed, and merely PMAA now forms a negatively charged corona (Figure 1b and e). Under physiological conditions (pH ∼ 7.4) both blocks are charged, leading to the formation of an intramicellar interpolyelectrolyte complex (*im*-IPEC) shell (Figure 1c and f). Hence, the micellar surface is patchy, featuring both charge neutral (*im*-IPEC) and

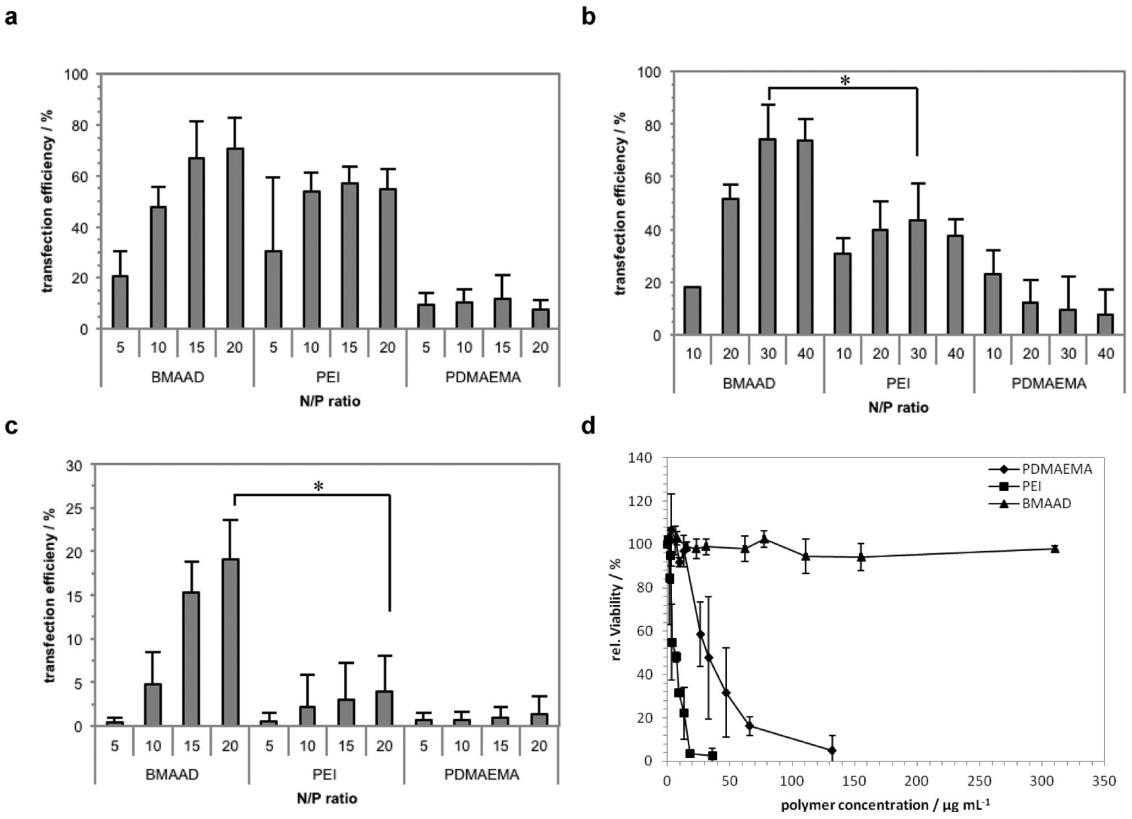

Figure 2. Transfection efficiencies of BMAAD, PEI_{570}, and $PDMAEMA_{191}$ for adherent HEK cells in serum-reduced (a) and serum-containing media (b) and human leukemia cells (c) at different N/P ratios. An EGFP (pEGFP-N1) was used as reporter gene. Cytotoxicity tests using L929 cells (d). Values represent the mean ± S.D; * represents a significant difference ($p < 0.01$).

cationic domains (the DP of PDMAEMA is higher than for the PMAA segment, resulting in an excess positive net charge). These IPEC patches may lead to an increased polycation density within parts of the corona, and this in turn favors the formation of patchy structures upon further complex formation.[27]

First, transfection studies of BMAAD with pDNA under serum-reduced conditions as well as with media containing 10% serum were performed with adherent HEK293 cells, using linear PEI_{570} (25 kDa) and $PDMAEMA_{191}$ (30 kDa) as comparison. The BMAAD micelles showed very high TE, even compared to PEI (BMAAD: 70 ± 12% at N/P 20; PEI: 55 ± 8% at N/P 20) under serum-reduced conditions (Figure 2a and Figure S1, Supporting Information). In contrast, linear PDMAEMA reaches only 12 ± 9% at N/P 15. This increased TE for adherent cells by using BMAAD micelles is in agreement with earlier studies on star-shaped PDMAEMA or micelles with a PDMAEMA corona.[28] In the presence of serum even superior results were obtained for BMAAD (74 ± 8% at N/P 30), comparable to Lipofectamine 2000,[29] whereas the TE decreased significantly for PEI (43 ± 7% at N/P 30; Figure 2b). The fact that BMAAD performs even better under serum conditions is remarkable as in general serum leads to unspecific interactions and lower TEs in case of cationic polymers.[28,30]

As the next step, the transfection of Jurkat T suspension cells with pDNA was evaluated. Figure 2c shows a TE of up to 19 ± 6% with polyplexes formed from BMAAD and pDNA (N/P 20), whereas both PEI and PDMAEMA show a significantly reduced TE, which is in agreement with literature.[31] The fact that BMAAD micelles reach a 5-fold higher TE compared to PEI highlights the potential of these structures as powerful transfection agents. It should be noted that the presence of PMAA within the *im*-IPEC shell does not decrease the TE. Moreover, transfection experiments under non static conditions (shaking) resulted in similar transfection efficiencies (Figure S8, Supporting Information). We also found no detectable cytotoxicity of BMAAD using sensitive L929 cells (Figure 2d) for concentrations up to 320 μg mL^{-1}, in contrast to PDMAEMA and PEI, which show IC_{50} values of 30 and 6 μg mL^{-1}, respectively. Even polyplexes of PEI/pDNA show lower values ($IC_{50} \sim 10$ μg mL^{-1}).[32] We propose that the PMAA block of BMAAD is responsible for the decreased cytotoxicity, without decreasing the TE in contrast to PEG.[10,33] Hence, the patchy micellar surface featuring cationic domains and neutral *im*-IPECs might serve as leverage to circumvent what is often called the "PEG-dilemma" (decreasing TE in the presence of a shielding PEG corona). The outstanding biocompatibility in combination with high TE values for

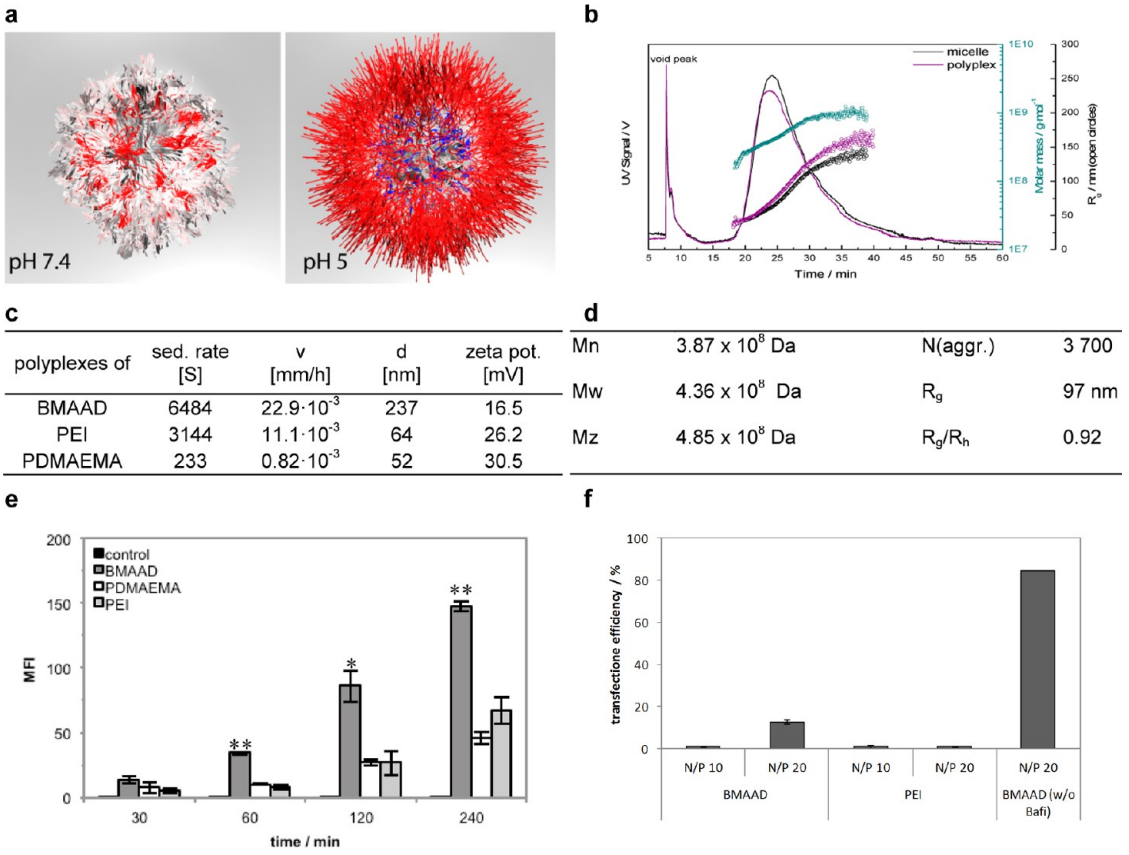

c

polyplexes of	sed. rate [S]	v [mm/h]	d [nm]	zeta pot. [mV]
BMAAD	6484	$22.9 \cdot 10^{-3}$	237	16.5
PEI	3144	$11.1 \cdot 10^{-3}$	64	26.2
PDMAEMA	233	$0.82 \cdot 10^{-3}$	52	30.5

d

Mn	3.87×10^8 Da	N(aggr.)	3 700
Mw	4.36×10^8 Da	R_g	97 nm
Mz	4.85×10^8 Da	R_g/R_h	0.92

Figure 3. Proposed surface characteristics of the BMAAD micelle (color code: red, positive charges/PDMAEMA; blue, negative charges/PMAA; white, neutral *im*-IPEC domains; a). Detailed characteristics of BMAAD micelles obtained by asymmetric flow field flow fractionation (AF4) at pH 7 (b, d). Sedimentation velocity, hydrodynamic diameter, and zeta potential of polyplexes formed at N/P 20 (c). Mean fluorescence intensity (MFI) of cells transfected with YOYO-1 labeled pDNA for indicated time points using BMAAD, PEI_{570}, and $PDMAEMA_{191}$ (e). Values represent the mean ± S.D; * represents a significant difference ($p < 0.05$) to PEI_{570} and $PDMAEMA_{191}$; ** represents a significant difference ($p < 0.01$) to PEI_{570} and $PDMAEMA_{191}$, # represents a significant difference ($p < 0.01$) to $PDMAEMA_{191}$. Transfection efficiencies using EGFP as reporter gene of BMAAD and PEI for adherent HEK cells treated with Bafilomycin (f).

BMAAD is impressive, as generally increases in efficiency are accompanied by higher cytotoxicity for transfection agents.[7,34] Thus, using an ampholytic triblock terpolymer containing both a cationic and an anionic segment allows constructing efficient nonviral gene delivery agents even though the cationic part, PDMAEMA, is usually regarded as being not very efficient.[35]

As such an outstanding performance was not anticipated for BMAAD, we were interested in the underlying mechanism. Therefore, all formed polyplexes were investigated with an ethidium bromide exclusion assay (EBA)[36] and dynamic light scattering (DLS) experiments. Both BMAAD and PDMAEMA show similar binding affinities to pDNA, but the values are lower compared to PEI (Figure S2, Supporting Information). This indicates the successful formation of polyplexes in all cases, as EBA only provides a qualitative assessment.[37] In addition, we performed a DNA gel migration assay, confirming the successful pDNA complexation at N/P 5 as no free pDNA could be detected (Figure S3, Supporting Information).

All polyplexes investigated exhibit a positive net charge at physiological pH, as shown in zeta-potential measurements (Figure 3c). Hydrodynamic diameters of 64 nm (PEI), 237 nm (BMAAD), and 52 nm (PDMAEMA) can be observed (Figure 3c). For BMAAD, the formed polyplexes are of comparable size as the "bare" micelles (212 nm),[26] which can be explained by a rather tight wrapping of pDNA around the particles.[38] pH-dependent surface characteristics of BMAAD are schematically presented in Figure 3a. At physiological pH (7.4) most of the PDMAEMA forms *im*-IPECs with PMAA (white), whereas a slightly positive surface charge is caused by excess protonated PDMAEMA (DP PDMAEMA > DP PMAA).[26] At endosomal pH (~5), PDMAEMA is highly protonated and stretched, whereas PMAA partially collapses. This is supported by pH-dependent zeta potential measurements. The appearance of neutral *im*-IPECs, cationic patches on the polyplex surface, and strong changes as a response to variations of the pH are also known from clusters of viral particles.[23−25]

The results could also be confirmed by asymmetric flow field-flow fractionation (AF4, Figure 3b), where an R_g of 97 nm was obtained for BMAAD and 111 nm for the corresponding polyplex; the obtained molar

masses were $M_n = 3.87 \times 10^8$ g mol^{-1} and $M_w = 4.36 \times 10^8$ g mol^{-1} for the micelle (Figure 3b and d). From the molar mass of the single triblock terpolymer (105 300 g mol^{-1}) the aggregation number can be calculated to roughly 3 700. Combining these results with the DLS data, the general ratio R_g/R_h, which provides information about the shape and the conformation of the sample, can be calculated. Typical values are 0.775 for a hard sphere, 1.0 for a soft sphere, or 1.78 for a monodisperse linear polymer chain in a good solvent.[39] In this study a value of 0.92 for the micelle and 0.94 for the corresponding polyplex were obtained, which both fit to the expected model of a soft sphere. With decreasing pH, the zeta potential as well as the hydrodynamic diameter increases from 16.5 mV and 237 nm to 30.3 mV and 420 nm (Figures 3c and 5). In addition, the stability of the BMAAD polyplexes in the presence of serum after 4 h was analyzed, and no significant changes could be observed (hydrodynamic diameter 230 nm), suggesting that no protein based aggregation takes place.

To achieve successful transfection in case of human leukemia cells, the binding affinity between polymer and pDNA, size, and zeta potential of the polyplexes is crucial. However, this has to be complemented by an enhanced recognition and uptake by the cells. The uptake is mainly influenced by the charge and a high concentration of polyplexes at the cell surface.[40] The latter can be accessed *via* the sedimentation rate of the polyplexes, as determined by analytical ultracentrifugation (AUC). Presumably, larger particles with higher sedimentation coefficients lead to an increased particle uptake in case of *in vitro* transfection.[41,42] Indeed, the trends observed from DLS studies (Figure 3c) can be confirmed, as polyplexes from BMAAD micelles revealed a higher sedimentation rate (6480 S) compared to PEI (3140 S) and PDMAEMA (230 S), most probably due to the rather dense PB core. This leads to longer and more intensive interactions between the cells and the polyplexes and, hence, an increased internalization.

To investigate the time-dependent cellular uptake of polyplexes, YOYO-1 labeled pDNA was used (Figure 3e and S8, Supporting Information). An enhanced uptake can be clearly achieved with BMAAD micelles compared to PEI or PDMAEMA. Already after 1 h the majority of cells internalized the labeled polyplexes with BMAAD, whereas 4 h are necessary in case of PEI (Figure S8, Supporting Information). Even more impressive, the overall amount of labeled pDNA taken up by all viable cells (mean fluorescence intensity, MFI, Figure 3e) is almost doubled for BMAAD at all indicated time points, demonstrating the enormous potential of these structures.

One previously identified bottleneck during transfection studies is the endosomal escape of polyplexes. For PEI, a rather high buffer capacity is known, causing the so-called proton sponge effect.[43] In contrast to PEI, PDMAEMA has lower buffer capacities,[26,44] which might explain a lower TE of linear PDMAEMA but not the high TE of BMAAD. Therefore, the behavior of BMAAD at endosomal pH ($\sim$ 5) was studied in more detail. Here, a rather stretched PDMAEMA corona and a partially collapsed PMAA shell can be anticipated.[26] The increased amount of positive charges lead to strong interactions with cellular membranes and, potentially, destabilization. This was confirmed both for the polymers and the polyplexes by a hemolysis assay at different pH values (Figure 4a and Figure S7, Supporting Information). While both PEI and PDMAEMA did not exhibit any hemolytic activity (Figure S7, Supporting Information), a strong pH-dependence with up to 30 and 8% at pH 5 was found for the BMAAD micelles and polyplexes, respectively. This supports our assumption that BMAAD destabilizes the endosomal membrane under acidic conditions and that the polyplex is released into the cytoplasm. The fact that this endosomal disruption is pH-dependent demonstrates the unique potential of such structures to react on subtle environmental changes and thereby induce endosomal escape.[45] To confirm the endosomal uptake and the necessity of acidification for an efficient transfection using BMAAD, transfections with bafilomycin were performed. Bafilomycin is known to inhibit the ATPases in the endosomes and therefore prevents acidification. The TEs of BMAAD and PEI are significantly decreased (Figure 3f) to 13 and 1%, respectively. It supports our assumption that endosomal pH facilitates destabilization and destruction of the endosomal membrane by shape/surface charge changes of the proposed BMAAD polyplexes. In addition, transfections were performed at 4 °C (Figure S8, Supporting Information), also significantly reducing the TE. To prove the fast and efficient endosomal escape, the colocalization of transported pDNA was investigated using confocal laser scanning microscopy (CLSM, Figure 4c). Therefore YOYO-1 labeled pDNA (green, Figure 4c) and LysoTracker Red (red, Figure 4c) were used to visualize the polyplexes as well as the late endosomes and lysosomes, respectively. Even after 1 h, a strong correlation of pDNA from PEI and PDMAEMA polyplexes and endosomes could be detected (yellow signal, Figure 4c) in contrast to BMAAD-based polyplexes. To verify the uptake of the BMAAD polyplexes *via* endocytosis, the colocalization of BMAAD polyplexes and early endosomes was demonstrated (Figure S8, Supporting Information).

Once the polyplexes are released into the cytoplasm, their dissociation is of great importance and was investigated using heparin, a negatively charged polysaccharide (Figure 4b). Typically, heparin concentrations of 10 U mL^{-1} are necessary to achieve a total release of pDNA from PEI-based polyplexes,[4] whereas 50 U mL^{-1} were needed for linear PDMAEMA, which is

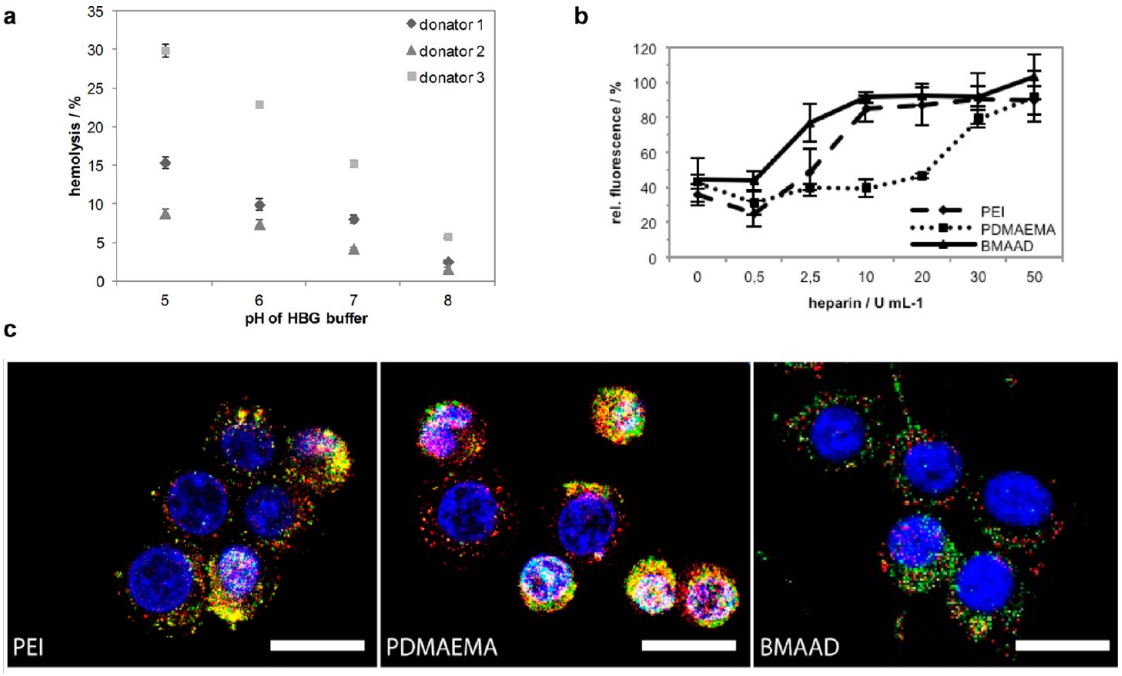

Figure 4. pH-dependent hemolysis assay of BMAAD of three different donators, each n = 3 (a). Dissociation assay of polyplexes formed at N/P 10 with increasing heparin concentrations (b). CLSM images of HEK cells transfected with indicated polymer based polyplexes and YOYO-1 labeled pDNA (green); late endosomes/lysosomes were stained with LysoTracker Red (red), and cell nuclei were stained with Hoechst 33342 (blue); each scale bar represents 20 μm; colocalization of pDNA and endosomal compartments are depicted in yellow (c).

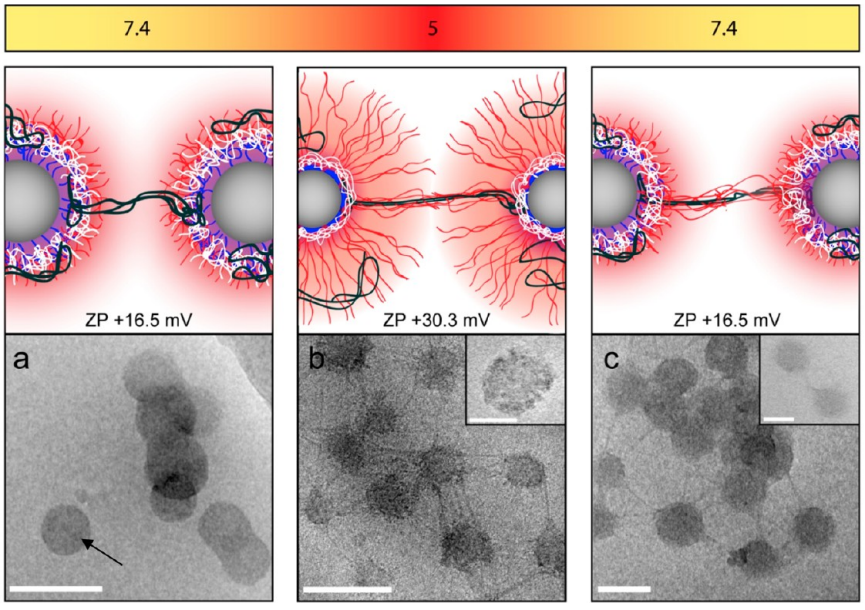

Figure 5. Schematic depiction of the proposed polyplex structure and the corresponding cryo-TEM micrographs at pH 7.4; the black arrow indicates the presence of *im*-IPECs (a), pH 5 (b), and pH 7.4 (c). Zeta potentials (ZP) of BMAAD polyplexes at pH 7.4 (16.5 mV) and pH 5 (30.3 mV). Color code: gray (PB), blue (PMAA), red (PDMAEMA), white (*im*-IPEC), and black (pDNA-polyplex). Scale bars indicate 200 nm and 50 nm in the insets.

a reason for the lower TE. Although BMAAD and PDMAEMA showed comparable binding affinities, the addition of only 10 U mL^{-1} of heparin led to an almost complete release of pDNA from BMAAD-based polyplexes. We attribute this to the PMAA block acting as a competing polyanion. In addition, the dissociation assay performed at pH 5 (Figure S5, Supporting Information) demonstrated a higher binding to pDNA, and thus, no polyplex dissociation in the endosome can be assumed.

The structure of the formed polyplexes was further investigated using cryo-TEM measurements at different pH-values (Figure 5). At pH 7.4, the BMAAD micelles are close to their isoelectric point,[26] and polyplex

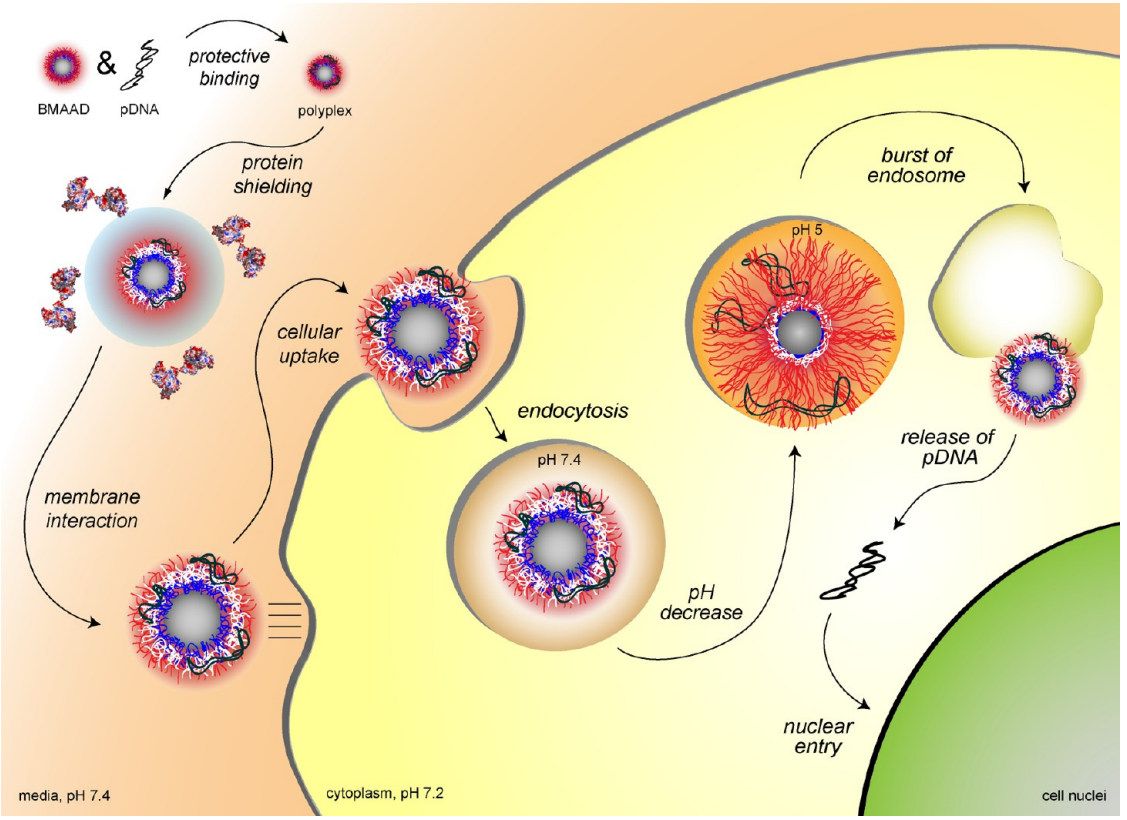

Figure 6. Schematic illustration of the proposed transfection mechanism for BMAAD-based polyplexes, with respect to the biological hurdles. The BMAAD micelle protects the genetic material (pDNA), prevents aggregation, and the cationic corona enables a fast and efficient cellular binding and uptake. Inside the endosomes, a decrease in pH leads to a swelling of the cationic corona and to a destabilization of the endosomal membrane. The release of the genetic material inside the cytoplasm is promoted by the middle block, PMAA, acting as a competing polyanion.

formation with pDNA leads to rather homogeneous structures of spherical shape (cryo-TEM, Figure 5a). The observed clustering can be explained by the rather low zeta potential of 16.5 mV. A decrease in pH within the endosome was simulated by the titration with dilute HCl until a pH of 5 was reached. This leads to full protonation and stretching of the PDMAEMA corona ($pK_a \sim 7.7$, zeta potential of 30.3 mV). Afterward, severe structural changes occur, as shown in Figure 5b: parts of the micellar core are covered by collapsed PMAA patches (blue), and in addition, the polyplexes formed of PDMAEMA (red) and pDNA (black) appear more dense and rigid, as seen in the protrusions connecting several micellar structures.[26]

These observations support our assumption of an endosomal burst occurring under these conditions and the data provided by hemolysis (Figure 4a). Subsequently, if the polyplex leaves the endosome, the pH within the cytoplasm rises to approximately 7.4, which was simulated for the same polyplex solution (Figure 5c). The cryo-TEM micrograph now shows polyplexes with the combined characteristics of Figure 5a and b: PMAA is resolubilized *via* deprotonation, leading to a more homogeneous overall appearance, and the rather rigid PDMAEMA/pDNA strands are still present, interconnecting several micelles. The latter can be explained by a closer look at the linear homopolymer of PDMAEMA, showing a rather strong binding between PDMAEMA and pDNA (linear PDMAEMA in Figure 4b). Since the polyplex is formed, neither an increase in pH (4 to 9, data not shown) nor the addition of heparin facilitated an easy release of pDNA. Hence, in the case of the BMAAD the negatively charged PMAA block acts as a competing polyelectrolyte, presumably reduces the binding between PDMAEMA and pDNA, and enables the release of genetic material in the cytoplasm. Comparable structural rearrangements induced by changes in pH have been reported for the Sindbis virus.[25]

So far, the use of BMAAD led to high TE and was accompanied by surprisingly low cytotoxicity and a facilitated release of pDNA. To highlight the advantage of this system, the proposed transfection mechanism with respect to the biological hurdles was schematically illustrated in Figure 6. After polyplex formation with pDNA, the internalization of the resulting structures crucially depends on the interaction with proteins and the cellular membrane. As we observed high transfection efficiency in the presence of serum proteins (Figure 2b) and no protein dependent aggregation, a good shielding behavior can be assumed. On the other hand, extremely fast cellular uptake

(Figure 3e and S8, Supporting Information) is caused by the presence of cationic surface patches, reminiscent to the surface clusters of certain viruses.[46,47] After internalization *via* endocytosis, prompt escape of the polyplexes from the endosome is facilitated by an increase in size and zeta potential due to protonation and swelling of the PDMAEMA segments (Figure 3a and Figure 5), avoiding both digestion and exocytosis (Figure 4c). In the cytoplasm, the release of the genetic material is supported by the presence of the middle block, PMAA, acting as a competing polyanion, resulting in an efficient expression of the reporter gene.

CONCLUSION

The successful design of powerful gene delivery agents imposes a range of bottlenecks,[15] but research efforts are justified by the potential applications within medicine and biotechnology.[48] Here, we presented a first study on the use of multicompartment micelles from stimuli-responsive triblock terpolymers as a new class of potential transfection agents. We propose that this might be the first step of a paradigm change for nonviral gene transfection agents as low cytotoxicity can be combined with outstanding TE for both adherent cells and rather hard-to-transfect human leukemia cells. In particular in the latter case, remarkable improvements compared to PEI and linear PDMAEMA were shown.

Detailed investigations of the underlying mechanism revealed a number of advantages for this system: the dense core of the BMAAD micelles leads to higher sedimentation rates and a superior cellular uptake. Furthermore, the interaction of two oppositely charged weak polyelectrolytes (PMAA and PDMAEMA) leading to *im*-IPECs and charge-neutral patches is to our opinion responsible for the reduced serum aggregation, unaffected viability, enhanced cellular uptake, and an improved pDNA release. In addition, under acidic conditions PDMAEMA provokes an increase in size and zeta potential, responsible for membrane destabilization and the release of the polyplex from the endosome.

Moreover, we believe that our results may aid in a profound understanding of the transfection mechanism of pDNA. Our mechanism was developed based on a combination of hemolysis data, cryo-TEM investigations (which provide structural insight into a model system), and microscopic images. All this is supported by pH-dependent zeta potential and size measurements.

In consequence, these effects render BMAAD a powerful advanced carrier for pDNA transfection studies, outperforming the "gold standard" PEI while maintaining superior biocompatibility. This work shows that by adopting certain design concepts from viruses (defined and responsive surface patches[23−25]) *via* the synthesis of well-defined block copolymers and the corresponding self-assembled aggregates superior control over (mainly) interface-dominated processes can be achieved. Of course, the next step would be to perform electron microscopy under cell culture conditions at different stages of the transfection process. To achieve this, we are currently working on strategies targeting the *in situ* immobilization of cells during different stages of transfection using fast gelation processes in aqueous media.

METHODS

Materials. Linear 25 kDa PEI was purchased from Polysciences (Eppelheim, Germany). Ethidium bromide solution 1% was purchased from Carl Roth (Karlsruhe, Germany). AlamarBlue, cell light early endosomes-RFP, BacMAM and YOYO-1 were obtained from Life Technologies (Darmstadt, Germany). If not stated otherwise, cell culture materials, cell culture media, and solutions were obtained from PAA (Pasching, Austria). Plasmid pEGFP-N1 (4.7 kb, Clontech, USA) was isolated using Qiagen Giga plasmid Kit (Hilden, Germany). All other chemicals were purchased from Sigma Aldrich (Steinhausen, Germany) and are of analytical grade or better and used without further purification. 2-Cyano-2-butyl dithiobenzoate (CBDB) was purchased from Aldrich and used without further purification. Azobis(isobutyronitrile) (AIBN, Aldrich) was recrystallized from methanol. 2-(Dimethylamino)-ethyl methacrylate (DMAEMA) was purchased from Aldrich and passed over a column filled with inhibitor remover prior to usage.

Synthesis of BMAAD Micelles. Synthesis and characterization of the BMAAD micelles were described previously.[26] Briefly, linear BTD triblock terpolymers were synthesized *via* sequential living anionic polymerization of the corresponding monomers in THF at low temperatures using *sec*-BuLi as initiator. Prior to the reaction, freshly distilled THF (600 mL) was treated with *sec*-BuLi at −20 °C, followed by stirring overnight at room temperature to produce alkoxides to stabilize the living polybutadienyl chain ends during the polymerization. In a typical reaction, 1,3-butadiene (20.5 mL, 13.3 g, 0.246 mol) was initiated with *sec*-BuLi (0.2 mL, 0.3 mmol) at −70 °C in THF and polymerized at −10 °C for 8 h. After polymerization of the first block, the living butadienyl chain ends were end-capped with 1,1-diphenylethylene (0.11 mL, 0.11 g, 0.6 mmol) for 1 h at −50 °C to attenuate the nucleophilicity. In this way, transfer reactions upon addition of the second monomer, *t*BMA, could be suppressed. Subsequently, *t*BMA (9.3 mL, 8.2 g, 0.057 mol) was added to the reaction mixture *via* syringe and stirred for 1 h at −40 °C. After polymerization of the second block, DMAEMA (20.2 mL, 18.9 g, 0.12 mol) was added *via* syringe.

Hydrolysis of the PtBMA Block. The BTD terpolymers were dissolved in dioxane at a concentration of 1 g L^{-1}. A spatula of the stabilizer 2,6-di-*tert*-butyl-*p*-cresol (BHT) and a 10-fold excess of hydrochloric acid relative to the ester moieties were added and the reaction mixture was refluxed at 120 °C for 24 h. Afterward, the excess of HCl was removed by dialysis against deionized water. After dialysis, micellar stock solutions in deionized water with concentrations of approximately 0.5 g L^{-1} were obtained. From these stock solutions changes in pH or salinity were performed by dialyzing against the corresponding buffer solutions.

Polyplex Preparation. Polyplexes of pDNA and polymers were prepared by mixing stock solutions of pDNA and polymers at a certain N/P ratio with 15 μg mL^{-1} of pDNA solution in HBG buffer (20 mM 4-(2-hydroxethyl) piperazine-1-ethanesulfonic acid (HEPES) and 5% (w/v) glucose, pH 7.2). Subsequently, the solutions were vortexed for 10 s at maximal speed and incubated at room temperature for 20 min.

Transfection of Adherent and Suspension Cells. HEK-293 cells (CRL-1573, ATCC) and Jurkat (TIB-152, ATCC) cells were maintained in RPMI 1640 culture medium, L929 cells (CCL-1, ATCC) in DMEM culture medium. Both media were supplemented with 10% fetal calf serum (FCS), 100 μg mL^{-1} of streptomycin, 100 IU mL^{-1} of penicillin, and 2 mM L-glutamine. Cells were cultivated at 37 °C in a humidified 5% CO_2 atmosphere.

For transfection of the adherent cell lines, cells were seeded at a density of 10^5 cells per well in 12-well plates one day before transfection. One hour prior to transfection, cells were rinsed with PBS and supplemented with 1 mL of OptiMEM (Life Technologies) or fresh serum-containing growth media (without antibiotics). Polyplexes (100 μL) were added to the cells, and the plates were incubated for 4 h in the incubator. Afterward, the supernatant was replaced by 1 mL of fresh growth medium, and the cells were further incubated for 20 h. For analysis, adherent cells were harvested by trypsinization. In the case of the Bafilomycin experiments, 175 nM Bafilomycin was added briefly before polyplex addition to OptiMEM.

For transfection of suspension cells (Jurkat), 0.25×10^5 cells were seeded in 0.25 mL of OptiMEM in 24-well plates, one hour prior to transfection. The polyplex solutions (50 μL) were added, and the plates were incubated for 4 h in the incubator. Afterward, 0.25 mL of growth medium were added, and the cells were incubated for further 20 h. For determination of the viability during flow cytometry, dead cells were identified *via* counterstaining with propidium iodide. The relative expression of EGFP fluorescence of 10^4 cells was quantified *via* flow cytometry using a Cytomics FC 500 (Beckman Coulter). For determination of the transfection efficiency viable cells expressing EGFP were gated. The experiments were performed independently three times. Confocal laser scanning microscopy (CLSM) was performed using as LSM510 (Carl Zeiss).

Plasmid DNA Labeling. For labeling of 1 μg pDNA, 0.026 μL of 1 M YOYO-1 solution was mixed with pDNA in 20 μL of pure water. The solution was incubated for 1 h at room temperature protected from light, before HBG was added to the used pDNA concentration described before. Polymers were added at the indicated N/P ratio, and the polyplex solution was treated as described before and added to the cells. After 4 h of incubation, the cells were harvested and 10% trypan blue was added to quench the outer fluorescence of cells and identify only those cells, which have taken up the genetic material. To determine the relative uptake of NPs, 10 000 cells were measured by flow cytometry, and the amount of viable cells showing YOYO-1 signal were gated. For measuring the mean fluorescence intensity, all viable cells were measured.

Cytotoxicity. The cytotoxicity was tested with L929 cells, as this sensitive cell line is recommended by ISO10993-5. In detail, cells were seeded at 10^4 cells per well in a 96-well plate and incubated for 24 h. No cells were seeded in the outer wells. Afterward, polymers at the indicated concentrations were added, and the cells were incubated at 37 °C for further 24 h. Subsequently, the medium was replaced by D-PBS and AlamarBlue as recommended by the supplier. After incubation for 4 h, the fluorescence was measured at Ex 570/Em 610 nm, with untreated cells on the same well plate serving as controls. The experiments were performed independently three times.

Analytical Ultracentrifugation. Analytical ultracentrifugation (AUC) was performed on a Beckman XL-I analytical ultracentrifuge (Krefeld, Germany). Experiments were carried out in double-sector aluminum centerpieces with an optical path length of 12 mm in a four holes rotor setup. Each cell was filled with 0.42 mL of solvent (HBG) and 0.4 mL of sample. A rotor speed between 1000 to 10 000 rpm was used, depending on the sample. The system was equilibrated for 40 min at 25 °C in the centrifuge. Sedimentation data were recorded by absorbance optics. Data analysis was done by the Sedfit software.[49]

Asymmetric Flow Field-Flow Fractionation (AF4). Asymmetric flow field-flow fractionation (AF4) was performed on an AF2000 MT System (Postnova Analytics, Landsberg, Germany) coupled to a UV (PN3211, 260 nm), RI (PN3150), and MALLS (PN3070, 633 nm) detector. The eluent is delivered by three different pumps (tip, focus, cross-flow), and the sample is injected by an autosampler (PN5300) into the channel. The channel has a trapezoidal geometry and an overall area of 31.6 cm^2. The nominal height of the spacer was 500 μm, and a regenerated cellulose membrane with a molar mass cutoff of 10 kDa was used as accumulation wall. All experiments were carried out at 25 °C, and the eluent was degassed water containing 0.02% NaN_3 to avoid bacterial growth. To prevent attractive interactions between the negative surface of the membrane and the positive charges in the corona of the micelle, the membrane surface was saturated by injection of 100 μg of pure PDMAEMA with the same procedure as for the micellar systems described below. Twenty microliters of samples were injected with an injection flow rate of 0.2 mL min^{-1} and a cross-flow rate of 0.9 mL min^{-1} for 7 min (detector flow rate was set to 1 mL min^{-1}). After a focusing step, the cross-flow rate was reduced under an exponential gradient (0.3) within 15 min to 0.05 mL min^{-1} and kept constant for 25 min. Afterward the cross-flow rate was reduced to 0 mL min^{-1} for 15 min to ensure complete elution. The refractive index increment for BMAAD was measured by manual injection of a known concentration directly into the channel without any focusing or cross-flow. Integration of the RI signal gives a dn/dc of 0.156 mL g^{-1}. For calculation of the molar mass and the radius of gyration the Berry plot was used.[50] All measurements were repeated 5 times.

Cryo-TEM Measurements. For cryo-TEM, 5 μL of the sample solution (in HBG) were applied to copper grids covered with a holey carbon film (Quantifoil R3.5/1 Micro Tools GmbH, Jena, Germany). The excess of the solution was automatically blotted with a filter paper (1 s), and the grid was then plunged rapidly into liquid ethane (−180 °C) in a cryobox (Carl Zeiss NTS GmbH). After removing excess ethane with a filter paper, the samples were transferred with a cryotransfer unit (Gatan 626-DH, Gatan GmbH, Munich, Germany) into the precooled cryoelectron microscope operated at 120 kV (Philips CM 120, Eindhoven, Netherlands) and viewed under low dose conditions with a bottom-mounted 1k CCD camera.

Conflict of Interest: The authors declare no competing financial interest.

Acknowledgment. We acknowledge funding from the Carl-Zeiss Foundation and the Thuringian Ministry for Education, Science, and Culture (TMBWK; grants #B514-09051, NanoConSens, and #B515-10065, ChaPoNano). E.B. gratefully acknowledges funding by the state of Bavaria through a BayEFG scholarship and support by the Elite Network of Bavaria. F. H. S. is grateful for a fellowship from the Fonds der chemischen Industrie (FCI). Moreover, we thank C. Fritzsche for hemolysis studies and Alamar Blue assays, A. Krieg for the synthesis of PDMAEMA, and A. Press for microscopic investigations. We would further like to thank reviewers #1 and #3 for helpful and critical comments.

Supporting Information Available: Additional experimental section. Flow cytometer analysis, ethidium bromide quenching assays, agarose gel migration assays, additional cryo-TEM measurements, heparin dissociation assays, polyplex stability in the presence and absence of serum, pH-dependent hemolysis assays, as well as further data regarding the uptake mechanism of the polyplexes. This material is available free of charge *via* the Internet at http://pubs.acs.org.

REFERENCES AND NOTES

1. Miyata, K.; Nishiyama, N.; Kataoka, K. Rational Design of Smart Supramolecular Assemblies for Gene Delivery: Chemical Challenges in the Creation of Artificial Viruses. *Chem. Soc. Rev.* **2012**, *41*, 2562–2574.
2. Ringsdorf, H. Hermann Staudinger and the Future of Polymer Research Jubilees—Beloved Occasions for Cultural Piety. *Angew. Chem., Int. Ed.* **2004**, *43*, 1064–1076.
3. Itaka, K.; Kataoka, K. Recent Development of Nonviral Gene Delivery Systems with Virus-like Structures and Mechanisms. *Eur. J. Pharm. Biopharm.* **2009**, *71*, 475–483.
4. Breunig, M.; Lungwitz, U.; Liebl, R.; Goepferich, A. Breaking up the Correlation Between Efficacy and Toxicity for Nonviral Gene Delivery. *Proc. Natl. Acad. Sci. U. S. A.* **2007**, *104*, 14454–14459.

5. Howard, K. A. Delivery of RNA Interference Therapeutics Using Polycation-Based Nanoparticles. *Adv. Drug Delivery Rev.* **2009**, *61*, 710–720.
6. Pergushov, D. V.; Müller, A. H. E.; Schacher, F. H. Micellar Interpolyelectrolyte Complexes. *Chem. Soc. Rev.* **2012**, *41*, 6888–6901.
7. Synatschke, C. V.; Schallon, A.; Jerome, V.; Freitag, R.; Müller, A. H. E. Influence of Polymer Architecture and Molecular Weight of Poly(2-(dimethylamino)ethyl methacrylate) Polycations on Transfection Efficiency and Cell Viability in Gene Delivery. *Biomacromolecules* **2011**, *12*, 4247–4255.
8. Majewski, A. P.; Schallon, A.; Jerome, V.; Freitag, R.; Müller, A. H. E.; Schmalz, H. Dual-Responsive Magnetic Core-Shell Nanoparticles for Nonviral Gene Delivery and Cell Separation. *Biomacromolecules* **2012**, *13*, 857–866.
9. Nguyen, J.; Xie, X.; Neu, M.; Dumitrascu, R.; Reul, R.; Sitterberg, J.; Bakowsky, U.; Schermuly, R.; Fink, L.; Schmehl, T.; *et al.* Effects of Cell-Penetrating Peptides and Pegylation on Transfection Efficiency of Polyethylenimine in Mouse Lungs. *J. Gene Med.* **2008**, *10*, 1236–1246.
10. Mishra, S.; Webster, P.; Davis, M. E. PEGylation Significantly Affects Cellular Uptake and Intracellular Trafficking of Nonviral Gene Delivery Particles. *Eur. J. Cell Biol.* **2004**, *83*, 97–111.
11. Behr, J. P. Synthetic Gene Transfer Vectors II: Back to the Future. *Acc. Chem. Res.* **2012**, *45*, 980–984.
12. Jordan, M.; Wurm, F. Transfection of Adherent and Suspended Cells by Calcium Phosphate. *Methods* **2004**, *33*, 136–143.
13. Keller, H.; Yunxu, C.; Marit, G.; Pla, M.; Reiffers, J.; Theze, J.; Froussard, P. Transgene Expression, But Not Gene Delivery, Is Improved by Adhesion-Assisted Lipofection of Hematopoietic Cells. *Gene Ther.* **1999**, *6*, 931–938.
14. Gary, D. J.; Puri, N.; Won, Y. Y. Polymer-Based siRNA Delivery: Perspectives on the Fundamental and Phenomenological Distinctions from Polymer-Based DNA Delivery. *J. Controlled Release* **2007**, *121*, 64–73.
15. Whitehead, K. A.; Langer, R.; Anderson, D. G. Knocking Down Barriers: Advances in siRNA Delivery. *Nat. Rev. Drug Discovery* **2009**, *8*, 129–138.
16. Moughton, A. O.; Hillmyer, M. A.; Lodge, T. P. Multicompartment Block Polymer Micelles. *Macromolecules* **2011**, *45*, 2–19.
17. Cui, H.; Chen, Z.; Zhong, S.; Wooley, K. L.; Pochan, D. J. Block Copolymer Assembly *via* Kinetic Control. *Science* **2007**, *317*, 647–650.
18. Gröschel, A. H.; Schacher, F. H.; Schmalz, H.; Borisov, O. V.; Zhulina, E. B.; Walther, A.; Müller, A. H. E. Precise Hierarchical Self-Assembly of Multicompartment Micelles. *Nat. Commun.* **2012**, *3*, 710.
19. Lodge, T. P.; Rasdal, A.; Li, Z.; Hillmyer, M. A. Simultaneous, Segregated Storage of Two Agents in a Multicompartment Micelle. *J. Am. Chem. Soc.* **2005**, *127*, 17608–17609.
20. Fukushima, S.; Miyata, K.; Nishiyama, N.; Kanayama, N.; Yamasaki, Y.; Kataoka, K. PEGylated Polyplex Micelles from Triblock Cationers with Spatially Ordered Layering of Condensed pDNA and Buffering Units for Enhanced Intracellular Gene Delivery. *J. Am. Chem. Soc.* **2005**, *127*, 2810–2811.
21. Lee, Y.; Miyata, K.; Oba, M.; Ishii, T.; Fukushima, S.; Han, M.; Koyama, H.; Nishiyama, N.; Kataoka, K. Charge-Conversion Ternary Polyplex with Endosome Disruption Moiety: A Technique for Efficient and Safe Gene Delivery. *Angew. Chem., Int. Ed.* **2008**, *47*, 5163–5166.
22. Oishi, M.; Sasaki, S.; Nagasaki, Y.; Kataoka, K. pH-Responsive Oligodeoxynucleotide (ODN)−Poly(Ethylene Glycol) Conjugate through Acid-Labile β-Thiopropionate Linkage: Preparation and Polyion Complex Micelle Formation. *Biomacromolecules* **2003**, *4*, 1426–1432.
23. Huang, Q.; Sivaramakrishna, R. P.; Ludwig, K.; Korte, T.; Bottcher, C.; Herrmann, A. Early Steps of the Conformational Change of Influenza Virus Hemagglutinin to a Fusion Active State: Stability and Energetics of the Hemagglutinin. *Biochim. Biophys. Acta* **2003**, *1614*, 3–13.
24. Dimitrov, D. S. Virus Entry: Molecular Mechanisms and Biomedical Applications. *Nat. Rev. Microbiol.* **2004**, *2*, 109–122.
25. Paredes, A. M.; Ferreira, D.; Horton, M.; Saad, A.; Tsuruta, H.; Johnston, R.; Klimstra, W.; Ryman, K.; Hernandez, R.; Chiu, W.; *et al.* Conformational Changes in Sindbis Virions Resulting from Exposure to Low pH and Interactions with Cells Suggest that Cell Penetration May Occur at the Cell Surface in the Absence of Membrane Fusion. *Virology* **2004**, *324*, 373–386.
26. Betthausen, E.; Drechsler, M.; Förtsch, M.; Schacher, F. H.; Müller, A. H. E. Dual Stimuli-Responsive Multicompartment Micelles from Triblock Terpolymers with Tunable Hydrophilicity. *Soft Matter* **2011**, *7*, 8880–8891.
27. Schacher, F.; Betthausen, E.; Walther, A.; Schmalz, H.; Pergushov, D. V.; Müller, A. H. E. Interpolyelectrolyte Complexes of Dynamic Multicompartment Micelles. *ACS Nano* **2009**, *3*, 2095–2102.
28. Schallon, A.; Synatschke, C. V.; Jerome, V.; Müller, A. H. E.; Freitag, R. Nanoparticulate Nonviral Agent for the Effective Delivery of pDNA and siRNA to Differentiated Cells and Primary Human T Lymphocytes. *Biomacromolecules* **2012**, *13*, 3463–3474.
29. Keeney, M.; Ong, S.-G.; Padilla, A.; Yao, Z.; Goodman, S.; Wu, J. C.; Yang, F. Development of Poly(β-amino ester)-Based Biodegradable Nanoparticles for Nonviral Delivery of Minicircle DNA. *ACS Nano* **2013**, *7*, 7241–7250.
30. Fischer, D.; Bieber, T.; Li, Y.; Elsasser, H. P.; Kissel, T.; Novel Non-Viral, A. Vector for DNA Delivery Based on Low Molecular Weight, Branched Polyethylenimine: Effect of Molecular Weight on Transfection Efficiency and Cytotoxicity. *Pharm. Res.* **1999**, *16*, 1273–1279.
31. Wang, D. A.; Narang, A. S.; Kotb, M.; Gaber, A. O.; Miller, D. D.; Kim, S. W.; Mahato, R. I. Novel Branched Poly-(ethylenimine)-Cholesterol Water-Soluble Lipopolymers for Gene Delivery. *Biomacromolecules* **2002**, *3*, 1197–1207.
32. Schallon, A.; Jerome, V.; Walther, A.; Synatschke, C. V.; Müller, A. H. E.; Freitag, R. Performance of Three PDMAEMA-Based Polycation Architectures as Gene Delivery Agents in Comparison to Linear and Branched PEI. *React. Funct. Polym.* **2010**, *70*, 1–10.
33. Vollrath, A.; Schallon, A.; Pietsch, C.; Schubert, S.; Nomoto, T.; Matsumoto, Y.; Kataoka, K.; Schubert, U. S. A Toolbox of Differently Sized and Labeled PMMA Nanoparticles for Cellular Uptake Investigations. *Soft Matter* **2013**, *9*, 99–108.
34. Kwok, A.; Hart, S. L. Comparative Structural and Functional Studies of Nanoparticle Formulations for DNA and siRNA Delivery. *Nanomedicine* **2011**, *7*, 210–219.
35. van de Wetering, P.; Moret, E. E.; Schuurmans-Nieuwenbroek, N. M.; van Steenbergen, M. J.; Hennink, W. E. Structure-Activity Relationships of Water-Soluble Cationic Methacrylate/Methacrylamide Polymers for Nonviral Gene Delivery. *Bioconjugate Chem.* **1999**, *10*, 589–597.
36. Waring, M. J. Complex Formation between Ethidium Bromide and Nucleic Acids. *J. Mol. Biol.* **1965**, *13*, 269–282.
37. Schallon, A.; Synatschke, C. V.; Pergushov, D. V.; Jerome, V.; Müller, A. H. E.; Freitag, R. DNA Melting Temperature Assay for Assessing the Stability of DNA Polyplexes Intended for Nonviral Gene Delivery. *Langmuir* **2011**, *27*, 12042–12051.
38. Alhoranta, A. M.; Lehtinen, J. K.; Urtti, A. O.; Butcher, S. J.; Aseyev, V. O.; Tenhu, H. J. Cationic Amphiphilic Star and Linear Block Copolymers: Synthesis, Self-Assembly, and *in Vitro* Gene Transfection. *Biomacromolecules* **2011**, *12*, 3213–3222.
39. Burchard, W. Solution Properties of Branched Macromolecules. *Polym. Sci.* **1999**, *143*, 113–194.
40. Florian, M. W. Production of Recombinant Protein Therapeutics in Cultivated Mammalian Cells. *Nat. Biotechnol.* **2004**, 1393–1398.
41. Luo, D.; Saltzman, W. M. Enhancement of Transfection by Physical Concentration of DNA at the Cell Surface. *Nat. Biotechnol.* **2000**, *18*, 893–895.
42. Tros de Ilarduya, C.; Sun, Y.; Duzgunes, N. Gene Delivery by Lipoplexes and Polyplexes. *Eur. J. Pharm. Sci.* **2010**, *40*, 159–170.

43. Akinc, A.; Thomas, M.; Klibanov, A. M.; Langer, R. Exploring Polyethylenimine-Mediated DNA Transfection and the Proton Sponge Hypothesis. *J. Gene Med.* **2005**, *7*, 657–663.
44. Cherng, J. Y. Investigation of DNA Spectral Conformational Changes and Polymer Buffering Capacity in Relation to Transfection Efficiency of DNA/Polymer Complexes. *J. Pharm. Pharm. Sci.* **2009**, *12*, 346–356.
45. Lee, Y.; Miyata, K.; Oba, M.; Ishii, T.; Fukushima, S.; Han, M.; Koyama, H.; Nishiyama, N.; Kataoka, K. Charge-Conversion Ternary Polyplex with Endosome Disruption Moiety: a Technique for Efficient and Safe Gene Delivery. *Angew. Chem., Int. Ed.* **2008**, *47*, 5163–5166.
46. Penin, F.; Combet, C.; Germanidis, G.; Frainais, P. O.; Deleage, G.; Pawlotsky, J. M. Conservation of the Conformation and Positive Charges of Hepatitis C Virus E2 Envelope Glycoprotein Hypervariable Region 1 Points to a Role in Cell Attachment. *J. Virol.* **2001**, *75*, 5703–5710.
47. Karlin, S.; Brendel, V. Charge Configurations in Viral Proteins. *Proc. Natl. Acad. Sci. U. S. A.* **1988**, *85*, 9396–9400.
48. Christie, R. J.; Nishiyama, N.; Kataoka, K. Minireview: Delivering the Code: Polyplex Carriers for Deoxyribonucleic Acid and Ribonucleic Acid Interference Therapies. *Endocrinology* **2010**, *151*, 466–473.
49. Schuck, P. Size-Distribution Analysis of Macromolecules by Sedimentation Velocity Ultracentrifugation and Lamm Equation Modeling. *Biophys. J.* **2000**, *78*, 1606–1619.
50. Andersson, M.; Wittgren, B.; Wahlund, K. G. Accuracy in Multiangle Light Scattering Measurements for Molar Mass and Radius Estimations. Model Calculations and Experiments. *Anal. Chem.* **2003**, *75*, 4279–4291.